

# EFFECTS OF INORGANICS ON THERMAL PROPERTY OF SILICONE RUBBER COMPOSITES

Jiuqiang Song<sup>1</sup>, Yan Qin<sup>1\*</sup>, Liangdian Liu<sup>1</sup>, Xi Zhang<sup>1</sup>, Zhixiong Huang<sup>1</sup>

<sup>1</sup>School of Materials Science and Engineering, Wuhan University of Technology, Wuhan, 430070, PR China, E-mail: songjq9@126.com

**Keywords:** Silicone rubber composites, Kaolin, Hydrated zinc borate, Thermal property.

## Abstract

In order to reduce the damage to life and property in our daily life, which caused by fire, fire retardant materials become the key point. As a kind of fire retardant material, ceramifiable silicone rubber composite has made a wide range of applications in the field, and is expected to have a further value. In this paper, The ceramic silicone rubber composite was prepared through using hydrated zinc borate as flame retardant and flux agent, kaolin as ceramic filler and high silica glass fiber as reinforcer. TGA-DTG analysis showed hydrated zinc borate increased the thermal decomposition temperature of the composite and improved the pyrolysis yield. B<sub>2</sub>O<sub>3</sub> and ZnO were generated from thermal decomposition of hydrated zinc borate, SiO<sub>2</sub> from Kaolin and silicone rubber. SEM images revealed that different structures were formed at different temperatures. B<sub>2</sub>O<sub>3</sub>, Al<sub>2</sub>O<sub>3</sub>, ZnO and SiO<sub>2</sub> played a important role in formation of ceramic. The network structure of the composite was more and more compact with the increasing of temperature from 600°C to 1000°C, which had a better protective effect. However, when temperature reached over 1200°C, the structure of the ceramic was destroyed and the composites were out of shape. In this paper, the theoretical study of the thermal performance and fire resistance of the ceramifiable silicone rubber composite could promote the application in the field of fire safety, so as to improve the safety factor for human life.

## 1 INTRODUCTION

Fire-resistant materials can achieve greater security under fire condition and ensure public safety from fire<sup>[1-3]</sup>. The traditional polymer materials being used as cable, when the fire happens, would be melted and release the toxic gas, which exposes the copper wire and cannot perform a very good fire retardant effect. The ceramifiable polymers were proposed by L.Hanu and his colleagues at first and achieved commercialized application successfully in 2004<sup>[4]</sup>. Ceramifiable polymers have the excellent performance like common polymers at room temperature and can form hard ceramic shell in fire or at temperature above 400°C. Silicone rubber composites have relatively lower heat release rates and minimal sensitivity to external heat flux in comparison to most organic polymers<sup>[2,5-7]</sup>. Eutectic reactions take place at high temperature between mineral fillers and degradation products of silicones, then the hard durable ceramic layer with porous structure is formed <sup>[8]</sup>. Fire-resistant composite of ceramifiable polymer has been studying by incorporating inorganic fillers, dispersant agent and other additives into the silicone polymer matrix <sup>[9, 10]</sup>. Thermal degradation of silicones has been thoroughly studied and the good thermal resistance property has been also proved <sup>[4, 11-13]</sup>.

Ceramifiable silicone rubber composites have the same excellent properties as ordinary silicone

rubber. Compared with the traditional organic polymers, there is no toxic substances during the combustion, and decomposition product, named  $\text{SiO}_2$ , can improve the flame retardant effect [14]. There are also many studies about effects of silicate mineral fillers on silicone rubber ceramization. For example, YB Cheng et al.[15-17] did a great deal of researches about ceramifiable mica/silicone rubber, frit-mica/silicone rubber and other silicone rubber composites. They found that the temperature was above  $800^\circ\text{C}$  if the ceramic reactions were accomplished by eutectic reactions between mica and pyrolysis products of silicones. While addition of frits could reduce the temperature of ceramic reaction. L.G.Hanu et al.[4] found the ultimate strength of the resultant ceramic residue improved after pyrolysis in air up to  $1100^\circ\text{C}$ . They confirmed that eutectic reaction and solidification process, being influenced by particle-size and chemical composition of the fillers, resulted to the strength improvement of the ceramic residue.

In the previous studies, many researchers focused their attention on the low temperature ceramization of silicone rubber composites, while ignoring the flame-retardant properties of the composites. Thus, in this paper, flame-resistance of ceramifiable silicone rubber was studied preliminarily. Effect of zinc borate as flame retardant and flux agent on the ceramifiable properties of silicone rubber composites was investigated also.

## 2 EXPERIMENTAL

### 2.1 Materials

Commercial methyl vinyl silicone rubber (MVQ) was produced by Chengdu Zhonghao Chenguang Technology Co. Ltd., China. The average molecular weights were about 350000~650000. The vinyl contents of the rubber was about 0.13~0.22. 2,5-Dimethyl-2,5-di(tert-butylperoxy)hexane (DBPH) was from Shanghai Jingchun Bio-Chem Technology Co. Kaolin was purchased from Guangzhou Zhenwei Chemical Technology Co. Ltd. Zinc borate ( $2\text{ZnO}\cdot 3\text{B}_2\text{O}_3\cdot 3.5\text{H}_2\text{O}$ , ZB) was also from Guangzhou Zhenwei Chemical Technology Co. Ltd. High silica glass fiber (GF) was purchased from Taizhou Tianma fiberglass Weaving Co. Ltd. The content of  $\text{SiO}_2$  was above 96%.

### 2.2 Preparation of Kaolin/ZB/MVQ composites

The silicone matrix, fillers (Kaolin and ZB) and vulcanizing agent DBPH were mixed using a two-roll open mill at room temperature. The samples were molded by press vulcanizer at  $170^\circ\text{C}$  with pressure of 10 MPa for 15 min. Then the platens were putted into air dry oven at  $200^\circ\text{C}$  for 2 hours for additional vulcanization. The formulations of rubber-composites were given in the Table 1.

| Sample code         | MVQ | Kaolin | ZB | GF | DBPH |
|---------------------|-----|--------|----|----|------|
| R <sub>40/0</sub>   | 100 | 40     | 0  | 0  | 2    |
| R <sub>40/10</sub>  | 100 | 40     | 10 | 0  | 2    |
| R <sub>40/15</sub>  | 100 | 40     | 15 | 0  | 2    |
| R <sub>40/20</sub>  | 100 | 40     | 20 | 0  | 2    |
| RF <sub>40/15</sub> | 100 | 40     | 15 | 4  | 2    |

Table 1 Chemical compositions (wt.%) of rubber composites

## 2.3 Sample pyrolysis

Pyrolysis of samples (100mm\*10mm\*4mm) was performed in a muffle furnace. In order to obtain the pyrolysis residues of different temperatures. Samples were heated from 50°C to 400°C, 600°C, 800°C, 1000°C or 1200°C at the heating rate of 10°C/min and kept at each temperature for 30 min.

## 2.4 Characterization

Thermal gravimetric analysis (TGA, STA449C/3/G, NETZSCH, Germany) was conducted to investigate the thermal stability of the samples under air gas conditions. Then a series of samples were heated at a rate of 10°C/min. The relative mass loss and heat change of the samples were recorded from room temperature to 1200°C.

Fourier transform infrared spectra (FTIR) was obtained in the range 4000-400cm<sup>-1</sup> at a resolution of 1cm<sup>-1</sup> by using a Nexus FTIR spectrophotometer (Thermo Nicolet, USA) employing the KBr pellet technique from room temperature to 400°C.

The crystal phases of the samples were identified by an X-ray diffraction (XRD) with a D8 ADVANCE diffractometer (Bruker) with Cu K $\alpha$  ( $\lambda=0.1542$  nm) radiation at a generator voltage of 40 kV and a generator current of 400mA. The scan was conducted from a  $2\theta$  angle of 10° to 80° with a step interval of 1°.

The morphology of the composite after ablation process was characterized by scanning electron microscopy (SEM, JSM-5610LV/\*, JOEL, Japan). The elemental distribution of the ceramic composite after ceramization was studied using energy dispersive spectroscopy (EDS, Zeiss Ultra Plus, Germany).

Bending strength of pyrolysis residues was performed using a Electronic Universal Material Testing Machine according to GB/T1449-2005.

## 3 RESULTS AND DISCUSSION

### 3.1 Thermal gravimetric analysis (TGA)

Fig.1 showed the TG-DTG curves of five different rubber composites.  $T_5$ ,  $T_{max}$  and pyrolysis yield at 1200°C were listed in Table 2.  $T_5$  and  $T_{max}$  was the temperature of 5% weight loss and peak degradation, respectively. It was clearly that the  $T_5$  and  $T_{max}$  of the R40/10, R40/15, R40/20 and RF40/15 composites were lower than those of R40/0. The low decomposition temperature indicated the reduction of thermal stability of the composites. It was mainly attributed to hydrated zinc borate which accelerated the process of thermal degradation of silicone rubber composites. Decomposition reaction of hydrated zinc borate happened due to heat absorption in 290~450°C and produced water, boric acid and boron oxide. In this process, heat of reaction was about 503KJ/Kg. And the weight of materials was reduced due to the gasification of water. On the other hand, with the continuous increase of temperature, the decomposition reaction would go on. Boron oxide started to soften at 350°C and turned to liquid at 500°C. So there was a tendency to break down the peak temperature. It found that the final residual amount of silicone rubber increased with the increase of hydrated zinc borate content.

It showed that hydrated zinc borate could improve pyrolysis yield and form perfect protective layer to cut off pervasion of external heat and decrease mass loss.

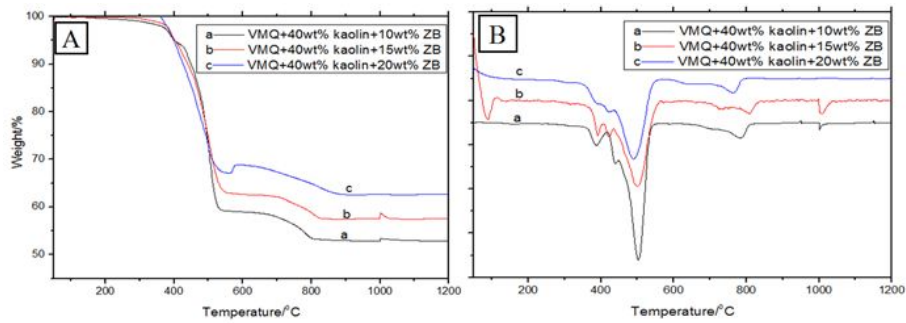


Fig. 1 TG and DTG curves for composites(A: TG curves, B: DTG curves)

| Sample code         | T <sub>5</sub> /°C | T <sub>max</sub> /°C | pyrolysis yield (wt%) |
|---------------------|--------------------|----------------------|-----------------------|
| R <sub>40/0</sub>   | 417                | 502.4                | 50.23                 |
| R <sub>40/10</sub>  | 402                | 502.3                | 53.34                 |
| R <sub>40/15</sub>  | 402                | 499.6                | 57.63                 |
| R <sub>40/20</sub>  | 398                | 492.4                | 63.63                 |
| RF <sub>40/15</sub> | 405                | 468.5                | 65.12                 |

Table 2 TGA results for thermal degradation of composites

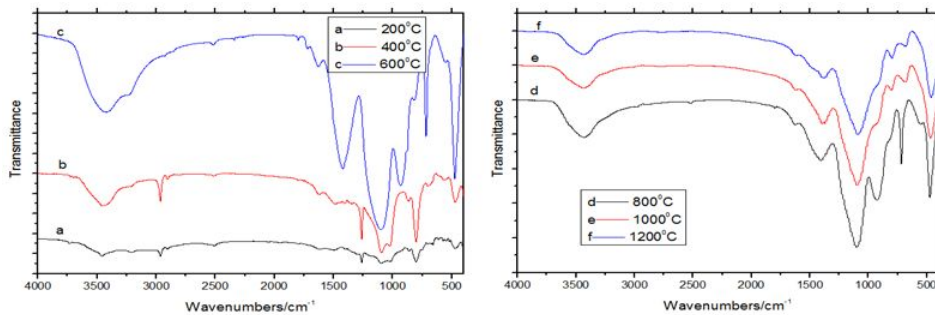


Fig. 2 FTIR spectra for ceramic layer

### 3.2 FTIR analysis

Fig. 2 showed there was the absorption peak of H<sub>2</sub>O at 400°C, and the peak became stronger at 600°C, which indicated decomposition reaction of hydrated zinc borate happened due to heat absorption, producing water. This was consistent with the previous conclusion. The “W” type absorption peak observed at 1100~1000cm<sup>-1</sup> was associated with the antisymmetric stretching and deformation vibration of Si-O-Si bond. The peak at 804cm<sup>-1</sup> was characteristic absorption peak of Si-O bond. The FTIR peak of Si-O-Si became weak and even disappeared at 600°C, which could be ascribed to the destruction of the network of silicone rubber, resulting in the crack of the Si-O-Si bond. However, the FTIR peak marked at 804cm<sup>-1</sup> at 1000°C was attributed to the stretching vibration of Si-O, suggesting the formation of SiO<sub>2</sub> in the layer. The FTIR peaks assigned to the vibrations of the methyl groups (Si-CH<sub>3</sub> stretching at 2964cm<sup>-1</sup>, Si-CH<sub>3</sub> wagging at 777cm<sup>-1</sup> and 1256cm<sup>-1</sup>) disappeared

in the ceramic layer before 600°C, which suggested the scission of Si-CH<sub>3</sub> in the silicone rubber side chains. The FTIR peak marked at 920cm<sup>-1</sup> was characteristic absorption peak of B-O bond. Moreover, the peaks at 600°C and 800°C were strong, which indicated B<sub>2</sub>O<sub>3</sub> was decomposition product of zinc borate.

### 3.3 XRD analysis

The XRD patterns for hydrated zinc borate were illustrated in Fig.3. It showed that hydrated zinc borate had a very obvious diffraction peak at room temperature and was typical monoclinic crystal.

As shown in Fig.4, a strong cubic zinc borate (ZnB<sub>2</sub>O<sub>4</sub>) diffraction peak appeared at 600°C, which hinted hydrated zinc borate released the crystal water and transformed into an anhydrous structure before 600°C. In addition, there were much more clear trenchant diffraction peaks at 800°C, and the characteristic peak of B<sub>2</sub>O<sub>3</sub> was observed at 15°, which indicated the B<sub>2</sub>O<sub>3</sub> was also obtained by the decomposition of hydrated zinc borate. However, the characteristic peaks of B<sub>2</sub>O<sub>3</sub> and ZnB<sub>2</sub>O<sub>4</sub> disappeared when the temperature was over 1000°C. There was only the diffraction peak of α-SiO<sub>2</sub> with hexagonal system structure. So hydrated zinc borate had been decomposed completely at 800°C.

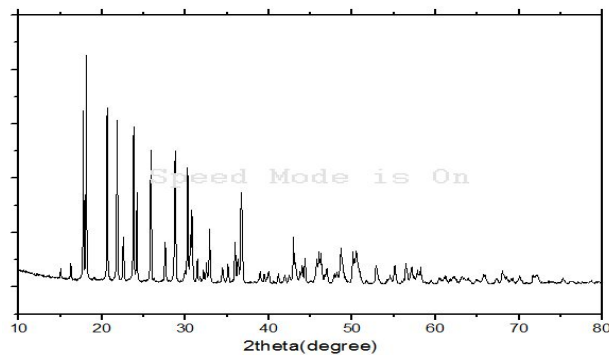


Fig. 3 The XRD patterns for hydrated zinc borate

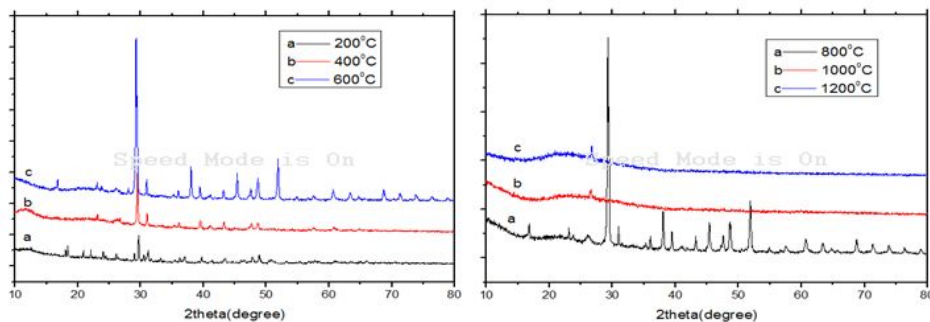


Fig. 4 The XRD patterns for decomposition products at different temperature

### 3.4 Microstructure of the composites

Fig.5 gave the SEM images of interior structure of no ceramization silicone composites. The morphology showed filler particles were uniformly distributed in the matrix and had good compatibility with silicone rubber. After calcination at 400°C, the composites was contracted, and micro cracks appeared on the surface of the materials due to release of crystalline water in

$2\text{ZnO}\cdot 3\text{B}_2\text{O}_3\cdot 3.5\text{H}_2\text{O}$  and scission of  $\text{Si-CH}_3$  from Fig.6. Zinc borate could be softened at  $350^\circ\text{C}$  and had fluidity above  $500^\circ\text{C}$  because of decomposition. The energy dispersive spectrometer (EDS) study of the distribution of elements after treatment at  $600^\circ\text{C}$  was illustrated in Fig. 7, which showed the major elements components of the materials were Si, O, Al and a little B. It could be speculated that  $\text{B}_2\text{O}_3$  was connected with the degradation products of rubber and the ceramic filler to a certain extent, which constituted the grid structure together.

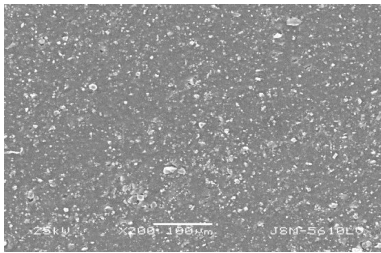


Fig. 5 Micro morphology of the original sample

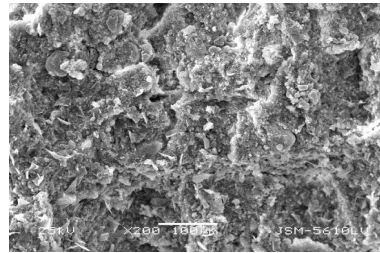


Fig.6 Micro morphology of the sample calcined at  $400^\circ\text{C}$

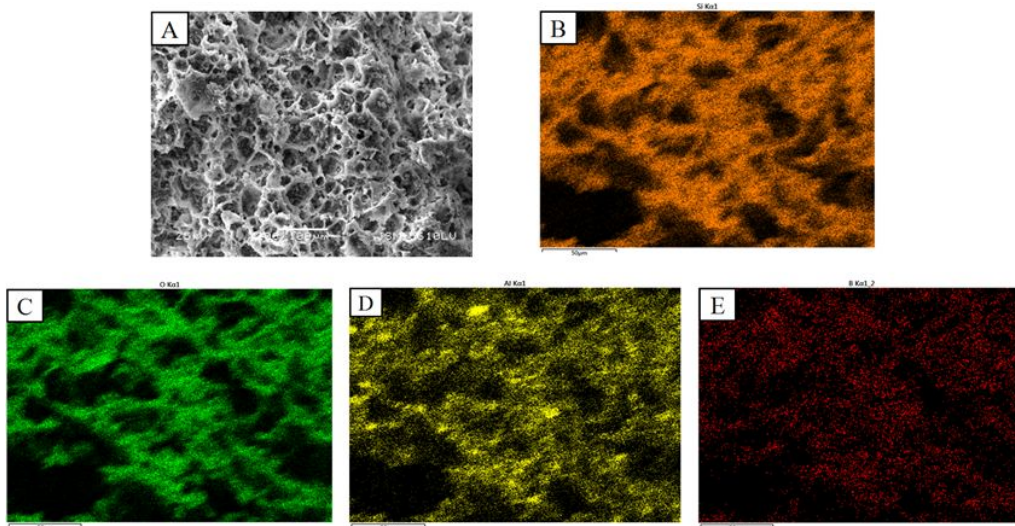


Fig. 7 Micro morphology and EDS scanning images of the sample calcined at  $600^\circ\text{C}$ (A: Micro morphology of the sample calcined at  $600^\circ\text{C}$ ; B, C, D, E: elements distribution of Si, O, Al, B, respectively)

Holes in the materials were smaller after calcination at  $800^\circ\text{C}$  than  $600^\circ\text{C}$  from Fig.8. The distribution of element B in the whole material was much more uniform and clearer. The structure was more complete and compact after ablation. This showed that the formation of liquid  $\text{B}_2\text{O}_3$  improved adhesion of the fillers and the matrix. At the same time, the strength of the ceramic material was improved obviously. The surface was also more complete and compact and there was no obvious crack appearance.

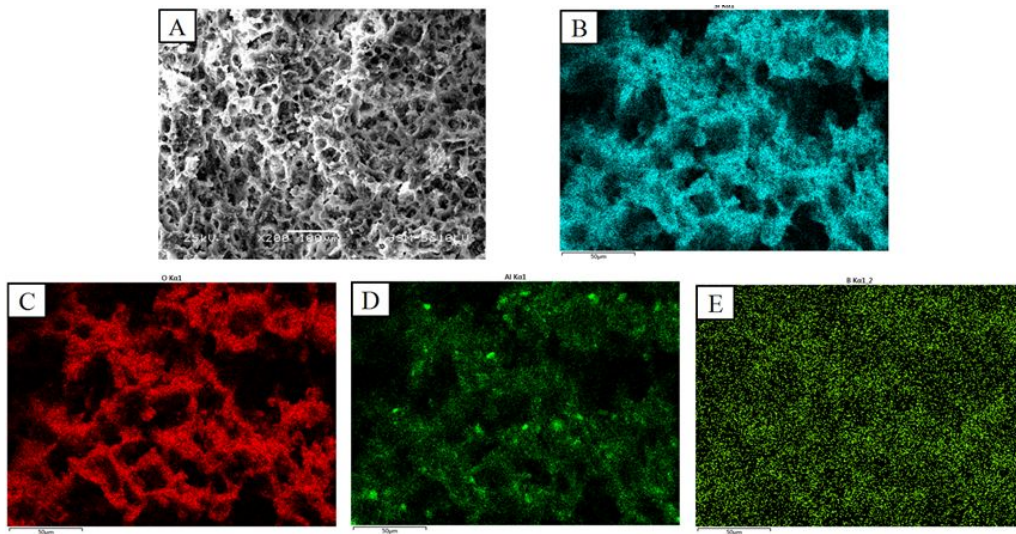


Fig. 8 Micro morphology and EDS scanning images of the sample calcined at 800°C(A: Micro morphology of the sample calcined at 800°C; B, C, D, E: elements distribution of Si, O, Al, B, respectively)

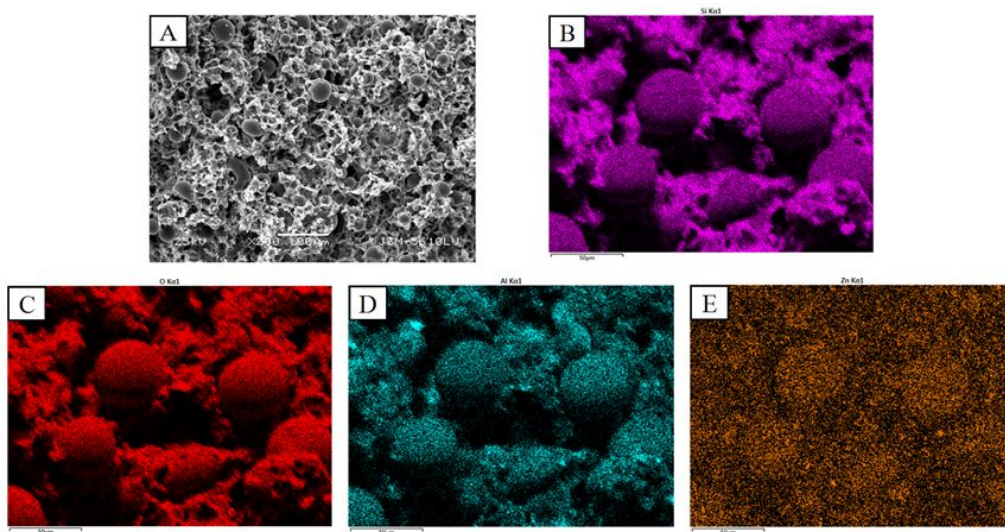


Fig. 9 Micro morphology and EDS scanning images of the sample calcined at 1000°C(A:Micro morphology of the sample calcined at 800°C; B, C, D, E: elements distribution of Si, O, Al, Zn, respectively)

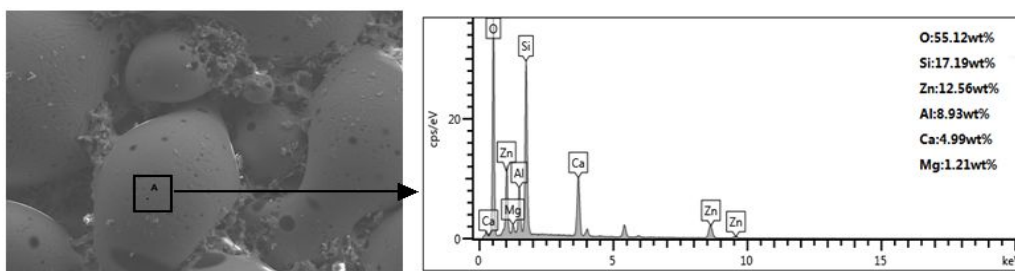


Fig. 10 result of EDS analysis of the sample calcined at 1000°C

In the Fig.9, there were a lot of molten ball drops which had uniform distribution after calcination at 1000°C. The EDS study of the distribution of elements showed the major elements components of the materials were Si, O, Al and Zn. The EDS study on molten ball drops showed in Fig.10. The result showed that a large number of Zn which derived from hydrated zinc borate existed in the spherical body except Si and O. So after adding hydrated zinc borate, molten ball drops would be formed and distributed in the composite evenly when the calcination temperature reached above 1000°C. There was almost no obvious hole in the whole silicone rubber material, and the strength of ceramic body reached the maximum. On the other hand, a hard dense ceramic protective layer was formed on the surface of composite, which isolated the internal material from the oxygen in the air to prevent the loss of quality and heat transfer.

However, when the calcination temperature was over 1200°C, the original shape of silicone rubber composite was lost. Viscous liquid with liquidity was produced. Fig. 11 showed the larger bubbles were generated in the matrix, which depressed the strength of the composites and lost inherent appearance shape.

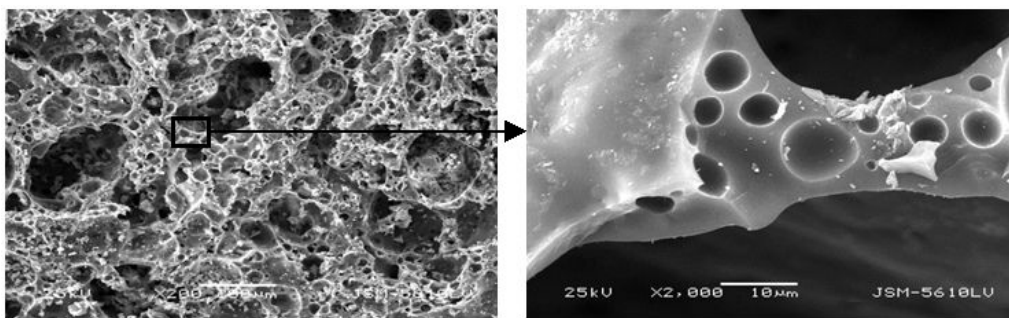


Fig. 11 Micro morphology of the sample calcined at 1200°C

### 3.5 Mechanical properties of the composites

Table.3 illustrated the bending strength of ceramic products had obvious change with the increase of sintering temperature. Before the composite had not been reinforced, the bending strength of ceramic products was relatively low. The bending strength reached the maximum when composite was calcined at 1000°C, that was 0.79MPa. While was reinforced by high silica glass fiber, the bending strength was obviously improved. With the increasing of sintering temperature, the bending strength was also increased because internal defects of silicone rubber composite were reduced. But when the sintering temperature continued to rise to 1200°C, the bending strength was reduced, which resulted from destruction of internal structure.

| Sample code         | Bending strength/Mpa |       |       |        |        |
|---------------------|----------------------|-------|-------|--------|--------|
|                     | 400°C                | 600°C | 800°C | 1000°C | 1200°C |
| R <sub>40/15</sub>  | 0.10                 | 0.39  | 0.54  | 0.79   | 0.47   |
| RF <sub>40/15</sub> | 0.11                 | 0.42  | 1.24  | 2.01   | 1.05   |

Table 3 Bending strength of samples calcined at different temperature

### 3.6 Ceramization Mechanism

The high temperature caused the degradation of the backbone of silicon rubber. Reaction of pyrolysis product and inorganic mineral fillers formed ceramic layer. First of all, the filler particles were distributed evenly and separated from each other in the silicone rubber matrix. No chemical reactions occurred. Then when the outside temperature began to rise, the crystal water was released from hydrated zinc borate because of the heat and the Si-O-Si bonds of the main chain in the silicone rubber matrix were broken to generate SiO<sub>2</sub>, attaching to the surface of composite. B<sub>2</sub>O<sub>3</sub> with low softening point was generated from decomposition of zinc borate. With the increasing of temperature, boron oxide melt little by little, which made Kaolin and silica bond together to form ceramics with a certain mechanical strength and self supporting structure. Finally, When the temperature was high enough, Kaolin was decomposed to generate Al<sub>2</sub>O<sub>3</sub> and SiO<sub>2</sub>. These oxides had eutectic reactions to produce a new liquid phase or solid phase. With the increasing of calcination temperature and time, the new liquid phase would diffuse into the matrix to form bonding among components like “liquid bridge”, which obtained ceramic protective layer with compact structure, stable shape and enough mechanical strength [15]. The protective layer effectively separated the external oxygen and the fire from the internal material, so as to prevent further heat dispersion and mass loss.

## 4 CONCLUSIONS

Adding hydrated zinc borate as flame retardant to the Kaolin/VMQ composites could significantly reduce the temperature of the ceramic transition and increase the mechanical strength of the material. The T<sub>5</sub> and T<sub>max</sub> of the composite had a certain degree of decline, while the pyrolysis yield had a significant improvement. B<sub>2</sub>O<sub>3</sub> was generated by the thermal decomposition of zinc borate at high temperature and participated in the formation of the material network structure. SiO<sub>2</sub>, as thermal decomposition product of silicone rubber, reacted with other fillers to form ceramic. SEM images revealed that different structures were formed in the ceramifiable silicone rubber composites at different temperatures. The network structure of the composite was more and more compact with the increasing of temperature from 600°C to 1000°C, which had a better protective effect. But when the temperature reached 1200°C, the structure of the ceramic was destroyed and the composite was out of shape.

## REFERENCES

- [1] J. Mansouri, C.A. Wood, K. Roberts, Y.B. Cheng, R.P. Burford, Investigation of the ceramifying process of modified silicone-silicate compositions, *J. Mater. Sci.* 42 (2007) 6046-6055.
- [2] S. Hamdani, C. Longuet, D. Perrin, J.M. Lopez-Cuesta, F. Ganachaud, Flame retardancy of silicone-based materials, *Polym. Degrad. Stab.* 94 (2009) 465-495.
- [3] A. Genovese, R.A. Shanks, Fire performance of poly(dimethyl siloxane) composites evaluated by cone calorimetry, *Compos. Part A Appl. Sci. Manuf.* 39 (2008) 398-405.
- [4] Hanu LG, Simon GP, Mansouri J, et al. Development of polymer Ceramic Composites for Improved Fire Resistance[J]. *Journal of Material Processing Technology*, 2004, 153-154: 401-407.

- [5] S. Hamdani-Devarenes, A. Pommier, C. Longuet, J.M. Lopez-Cuesta, F. Ganachaud, Calcium and aluminium-based fillers as flame-retardant additives in silicone matrices II. Analyses on composite residues from an industrial-based pyrolysis test, *Polym. Degrad. Stab.* 96 (2011) 1562-1572.
- [6] S. Hamdani-Devarenes, C. Longuet, R. Sonnier, F. Ganachaud, J.M. Lopez-Cuesta, Calcium and aluminum-based fillers as flame-retardant additives in silicone matrices. III. Investigations on fire reaction, *Polym. Degrad. Stab.* 98 (2013) 2021-2032.
- [7] F. Guastavino, A. Ratto, M. Celentano, A. Zucchelli, P. Michelato, Comparison between different electric signal fire resistant cables behaviour during fire tests, in: 2008 Annual Report Conference on Electrical Insulation and Dielectric Phenomena, 2008, pp. 103-106.
- [8] Anyszka R, Bieliński DM, Pedzich Z, Szumera M. Influence of surfaces of modified montmorillonites on properties of silicone rubber-based ceramizable composites[J]. *Journal of Thermal Analysis and Calorimetry*, 2015, 119(1):111-121.
- [9] A. Bacher, Silicone rubber used for fire safety and fire retardant cables, in: 2010 45th International Universities Power Engineering Conference (UPEC 2010), 2010, p. 4.
- [10] K. Hayashida, S. Tsuge, H. Ohtani, Flame retardant mechanism of polydimethylsiloxane material containing platinum compound studied by analytical pyrolysis techniques and alkaline hydrolysis gas chromatography, *Polymer* 44 (2003) 5611-5616.
- [11] L.G. Hanu, G.P. Simon, Y.B. Cheng, Thermal stability and flammability of silicone polymer composites, *Polym. Degrad. Stab.* 91 (2006) 1373-1379.
- [12] L. Yu, S.T. Zhou, H.W. Zou, M. Liang, Thermal stability and ablation properties study of aluminum silicate ceramic fiber and acicular wollastonite filled silicone rubber composite, *J. Appl. Polym. Sci.* (2014) 131.
- [13] D. Zhuo, A. Gu, G. Liang, J-t Hu, L. Cao, L. Yuan, Flame retardancy and flame retarding mechanism of high performance hyper branched polysiloxane modified bismaleimide/cyanate ester resin, *Polym. Degrad. Stab.* 96 (2011) 505-514.
- [14] Hshieh FY. Shielding effects of silica-ash layer on the composition of silicones and their possible applications on the fire retardancy of organic polymers[J]. *Fire and Materials*, 1998, 22(2): 69-76.
- [15] Mansouri J, Burford R, Cheng YB. Pyrolysis behaviour of silicone-based ceramifying composites[J]. *Materials Science and Engineering A-Structural*, 2006, 425(1-2): 7-14.
- [16] Mansouri J, Burford R, Cheng YB, et al. Formation of strong ceramified ash from silicone-based compositions[J]. *Journal of Materials Science*, 2005, 40(21): 5741-5749.
- [17] Hanu LG, Simon GP, Cheng YB. Preferential orientation of muscovite in ceramifiable silicone composites[J]. *Materials Science and Engineering A-Structural*, 2005, 398(1-2): 180-187.